Environmental Modelling & Software xxx (2010) 1–11

Contents lists available at ScienceDirect

Environmental Modelling & Software

journal homepage: www.elsevier.com/locate/envsoft

Uncertainty propagation in puff-based dispersion models using polynomial chaos

Umamaheswara Konda [a,*], Tarunraj Singh [a], Puneet Singla [a], Peter Scott [b]

[a] Department of MAE, University at Buffalo, Buffalo, NY, USA
[b] Department of CSE, University at Buffalo, Buffalo, NY, USA

ARTICLE INFO

Article history:
Received 5 October 2009
Received in revised form
1 April 2010
Accepted 6 April 2010
Available online xxx

Keywords:
Atmospheric dispersion
Polynomial chaos
Uncertainty propagation
Sensitivity analysis
Non-Gaussian distributions

ABSTRACT

Atmospheric dispersion is a complex nonlinear physical process with numerous uncertainties in model parameters, inputs, source parameters, initial and boundary conditions. Accurate propagation of these uncertainties through the dispersion models is crucial for a reliable prediction of the probability distribution of the states and assessment of risk. A simple three-dimensional Gaussian puff-based dispersion model is used as a test case to study the effect of uncertainties in the model parameters and initial conditions on the output concentration. A polynomial chaos based approach is used to numerically investigate the evolution of the model output uncertainties due to initial condition and parametric uncertainties. The polynomial chaos solution is found to be an accurate approximation to ground truth, established by Monte Carlo simulation, while offering an efficient computational approach for large nonlinear systems with a relatively small number of uncertainties.

1. Introduction

Real-time detection, tracking, hindcasting, nowcasting and forecasting of chemical, biological and radiological (CBR) releases are important for fast response to CBR leakages and attacks. Atmospheric dispersion models are used to track the evolution of the releases and assess the impact of the exposure to potentially harmful contaminants over space and time. They enable acquisition of useful knowledge about the hazardous releases due to chemical incidents like the Bhopal toxic gas release disaster in 1984 and radiological incidents like the Chernobyl nuclear accident in 1986 (National Research Council (U.S.), 2003). Uncertainty analysis of models is recommended as an integral part of any risk assessment to quantify the degree of confidence in the estimate of risk and is particularly significant in CBR applications (IAEA, 1989; Rao, 2005), since impact to life and property may be catastrophic.

Dispersion involves transport (advection) and diffusion of the target species released into the atmosphere. Dispersion modeling uses mathematical formulations to characterize the atmospheric processes that disperse a pollutant emitted by a source. Various atmospheric dispersion models have been developed to estimate the downwind concentration of the releases, some of which are addressed in the (Environmental Protection Agency) EPA's Guideline on Air Quality Models (EPA, 2005). Long-range atmospheric dispersion models, which emphasize regional and continental scales (Whelpdale, 1991), calculate concentration values over a relatively short period of time (hours or days). Models of this type are often used to deal with accidental CBR releases (EUJRC, 2004). Two categories of long-range atmospheric dispersion models can be distinguished, Eulerian and Lagrangian. Eulerian models describe the dispersion of pollutants in a fixed frame of reference (fixed with respect to a point on the earth surface). In Lagrangian models, the evolution of a pollutant air parcel (or puff) is described relative to a mobile reference system associated with the puff from its initial position as it moves along its trajectory. In the Lagrangian approach, diffusion, transformation and removal calculations are performed for the moving puffs (Whelpdale, 1991). The Lagrangian models have been widely used for problems of regional-to-continental scales. RIMPUFF (RIso Mesoscale PUFF model) (Thykier-Nielsen et al., 1999), CALPUFF (CALifornia PUFF model) (ASG-TRC, 2003), SCIPUFF (Second-order Closure Integrated PUFF model) (Sykes et al., 1998) are examples of puff-based atmospheric dispersion models for calculating the concentration and doses resulting from the dispersion of airborne materials.

Dispersion is a complex nonlinear physical process with numerous uncertainties in model parameters, inputs, source parameters, initial and boundary conditions. Accurate propagation of these uncertainties through the models is crucial for a reliable prediction of the probability distribution of the states and assessment of risk. Uncertainty propagation in various kinds of dynamical models has been studied extensively in various fields. Most of the

* Corresponding author.
E-mail address: venkatar@buffalo.edu (U. Konda).

1364-8152/$ – see front matter © 2010 Published by Elsevier Ltd.
doi:10.1016/j.envsoft.2010.04.005

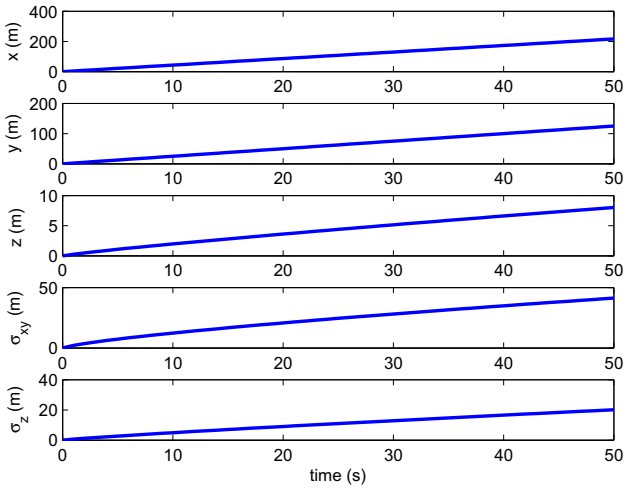

Fig. 1. Evolution of puff states.

methods incorporate linear approximations to nonlinear system response, or involve propagating only a few moments (often, just the mean and the covariance) of the distribution. Adjoint models (Errico, 1997) and parametric differentiation belong to this class and are widely used in sensitivity analysis of the models. These work well if there is adequate local linearity. Another class of methods, often used with models involving nonlinearities, are the various sampling techniques (Helton et al., 2006). The uncertainty distributions are taken into account by sampling values from known or approximated distributions and the model is run repeatedly for those values to obtain a sample distribution of the outputs. A Gaussian mixture based approach is proposed in (Terejanu et al., 2008) for accurate uncertainty propagation through nonlinear dynamical systems due to uncertain initial conditions. Surveys of the various methods used for uncertainty analysis in dispersion and transport models can be found in (Rao, 2005; Isukapalli, 1999).

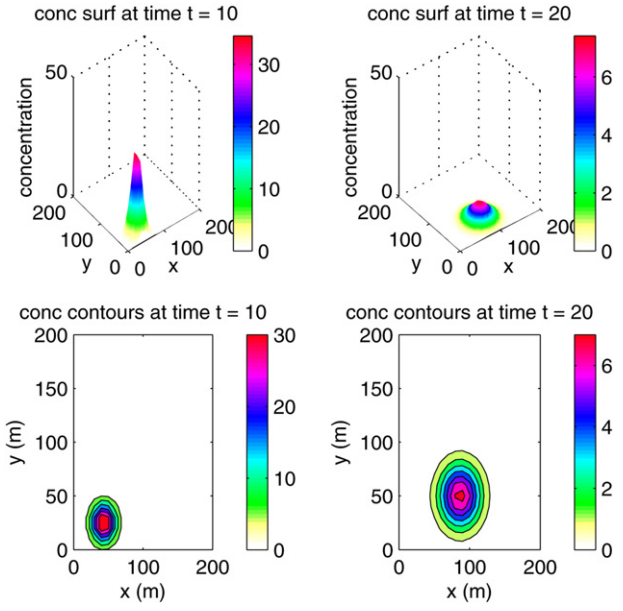

Fig. 2. Evolution of concentration.

The present work applies generalized polynomial chaos theory (Xiu and Karniadakis, 2002) to efficiently approximate the solution of a nonlinear dynamical model with parametric uncertainties. Polynomial chaos is a term originated by Norbert Wiener in 1938 (Wiener, 1938), to describe the members of the span of Hermite polynomial functionals of a Gaussian process. According to the Cameron–Martin Theorem (Cameron and Martin, 1947), the Fourier–Hermite polynomial chaos expansion converges, in the L^2 sense, to any arbitrary process with finite variance (which applies to most physical processes). This approach is combined with the finite element method to model uncertainty in (Ghanem and Spanos, 1991). This has been generalized in (Xiu and Karniadakis, 2002) to efficiently use the orthogonal polynomials from the Askey-scheme to model various probability distributions. The polynomial chaos approach has been applied in modeling uncertainties in multibody dynamical systems (Sandu et al., 2006), environmental and biological systems (Isukapalli et al., 1998), structural mechanics (Ghanem and Red-Horse, 1999) and computational fluid dynamics (Najm; Knio and Le Maître, 2006). This approach has been recently applied for uncertainty quantification and apportionment studies on an Eulerian air quality model (Cheng and Sandu, 2009). Monte Carlo techniques have been applied in (Rood et al., 2001) to obtain stochastic estimates of exposure and cancer risk, due to parametric uncertainties in a Lagrangian Gaussian-puff dispersion model. The present work involves the propagation of parametric and initial condition uncertainty through a nonlinear puff-based Lagrangian dispersion model, using polynomial chaos. Gaussian puff-based models (Thykier-Nielsen et al., 1999; Holmes and Morawska, 2006)] of this sort are often used to make fast release concentration predictions, in which a series of Gaussian shaped puffs (pollutant atmospheric parcels with a Gaussian distribution of the concentration field for each puff) are released at the sources and propagated in the atmosphere.

In this work, a representative three-dimensional nonlinear Gaussian puff-based dispersion model is used to examine the effects of diffusion parametric uncertainties on the solution. The model is introduced and its dynamics are described in Section 2. The polynomial chaos approach is described in Section 3. Then, the uncertainty propagation is considered for uncertainties in diffusion parameters for two important cases in the target applications: normal and uniform distributions. The selection of these two distributions is solely for the purpose of illustrating the generality of the proposed approach. The selection of the Gaussian distribution permitted using the error propagation approach with the linearized model to be compared to the proposed approach. The results of numerical trials are discussed in Section 4. Section 5 includes some concluding remarks and thoughts for future work.

2. Dispersion model

The atmospheric dispersion model used in this work is based on the RIMPUFF (Thykier-Nielsen et al., 1999) (Riso Mesoscale PUFF) model which was designed to calculate the concentration and doses resulting from the dispersion of airborne radioactive particles. It is a Lagrangian mesoscale atmospheric dispersion puff model, which applies both to homogeneous and inhomogeneous terrain with moderate topography on a horizontal scale of up to 50 km, and responds to changing (non-stationary) meteorological conditions. The model simulates the time-varying release (emission) of airborne materials by sequentially releasing a series of Gaussian shaped puffs at a fixed rate on a specified grid. The amount of airborne material allocated to individual puffs equals the current release rate multiplied by the elapsed time between puff releases. At each time step, the model advects, diffuses and deposits the individual puffs according to local meteorological and

Please cite this article in press as: Konda, U., et al., Uncertainty propagation in puff-based dispersion models using polynomial chaos, Environ. Model. Softw. (2010), doi:10.1016/j.envsoft.2010.04.005

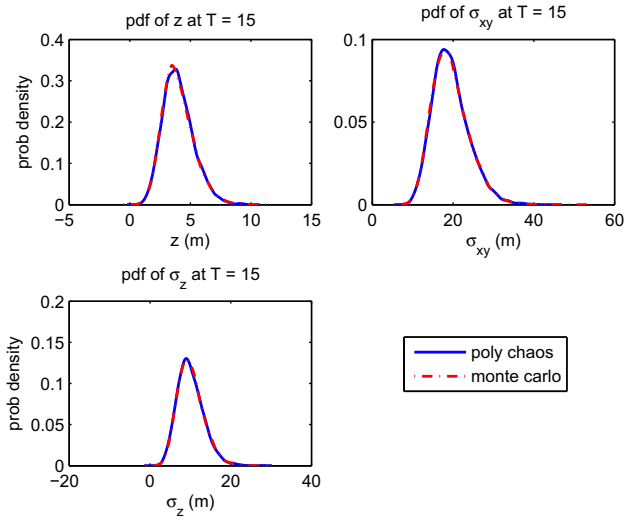

Fig. 3. *pdf* of uncertain states for normally distributed uncertainties.

physico-chemical parameter values. This model is used as a basis to design the present simple dispersion model to study the effects of parametric uncertainty on the solution.

2.1. Gaussian puff characteristics

The concentration distribution in each puff is Gaussian in three-dimensional physical space. Its mean represents the location of the puff center, and the standard deviations scale the size of the puff in the three spatial directions. For convenience, the standard deviation σ_x in the downwind direction is made equal to the standard deviation σ_y in the crosswind direction and is denoted by σ_{xy}. The activity Q of the puff is assumed to be constant, that is, deposition and species conversion are not modeled.

Each Gaussian puff has five scalar parameters which vary with time: $[X, Y, Z, \sigma_{xy}, \sigma_z]$, where

$X = [X, Y, Z]^T$, Centroid of the Gaussian puff

σ_{xy} = Puff size in x and y directions (std. deviation)

σ_z = Puff size in z-direction

The concentration c at a grid point $x_g = [x_g, y_g, z_g]^T$, at each time step, is calculated by summing the contributions of all the puffs at that instant.

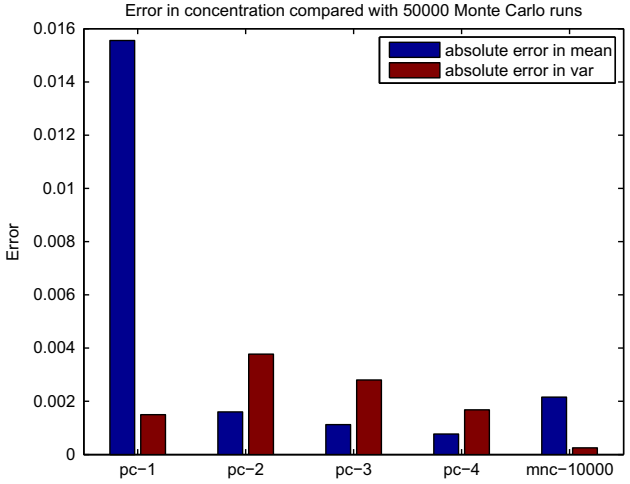

Fig. 4. Absolute error in estimated concentration mean and variance at $Xg = [20,10,0]$ for $T = 15$.

$$c(x_g) = \sum_{j=1}^{N} \frac{Q_j}{\sqrt{(2\pi)^3 \left|\sum_j\right|}} e^{\left[-\frac{(x_j - x_g)^T \sum_j^{-1} (x_j - x_g)}{2}\right]} \quad (1)$$

where N is the number of puffs and the covariance matrix is given by:

$$\sum_j = \begin{bmatrix} \sigma_{xy} & 0 & 0 \\ 0 & \sigma_{xy} & 0 \\ 0 & 0 & \sigma_z \end{bmatrix}$$

2.2. Puff dynamics

The advection and diffusion of each puff take place according to local meteorological parameter values. In this model, the advection of each puff is calculated according to the surface wind vector, u at the puff center and the time step, ΔT used to determine the next position of the puff center. Wind shear will cause the puff height to increase when the vertical diffusion σ_z increases. Plume rise due to heat content, buoyancy, release momentum and other effects is ignored for the present simple model, which is given by the ordinary difference equations:

$$\begin{aligned} X_{k+1} &= X_k + u_X \Delta T \\ Y_{k+1} &= Y_k + u_Y \Delta T \\ Z_{k+1} &= \sqrt{Z_k^2 + \tfrac{\sigma_z - \sigma_z}{2\pi}} \\ \text{where, } \mathbf{u} &= [u_X, u_Y]^T \text{at} [X_k, Y_k]^T \end{aligned} \quad (2)$$

u_X, u_Y being the X and Y components of the wind vector. Expansion with time of a single puff is fundamentally related to the relative diffusion process. It is computed from simultaneous measurements or specifications of the atmospheric turbulence intensity and/or stability in the dispersion area. For the current model, standard plume dispersion information is used. Pasquill parameterization, using a modified Karlsruhe–Jülich system (Thykier-Nielsen et al., 1999), is employed. These parameters can be used to describe puff growth in a constant wind field scenario (Zannetti, 1990) which we consider in the present work. This parameterization is valid for limited cases of near ground level releases and dispersion over flat terrains. The growth of each puff is described by

$$\begin{aligned} \sigma_{xyk+1} &= p_y s_{k+1}^{q_y} \\ \sigma_{zk+1} &= p_z s_{k+1}^{q_z} \\ \text{where, } s &= \text{downwind distance given by,} \\ s_{k+1} &= s_k + \sqrt{u_X^2 + u_Y^2}\Delta T \\ &= \left(\tfrac{\sigma_{xyk}}{p_y}\right)^{1/q_y} + \sqrt{u_X^2 + u_Y^2}\Delta T \\ p_y, q_y, p_z, q_z &= \text{stability dependent parameters} \\ &\quad (\text{Karlsurhe} - \text{Julich diffusion coefficients}) \end{aligned} \quad (3)$$

Deposition and target species chemical reactivity are neglected for the present model and hence the mass of each puff remains constant during the dispersion process.

3. Polynomial chaos

The polynomial chaos theory is applied for the solution of a system of difference equations. A dynamical system with uncertainties represented by a set of equations with stochastic parameters, can be transformed into a deterministic system of equations in the coefficients of a series expansion using this approach. The development in this section largely follows (Ghanem and Spanos, 1991) and (Xiu and Karniadakis, 2002). The basic goal of the

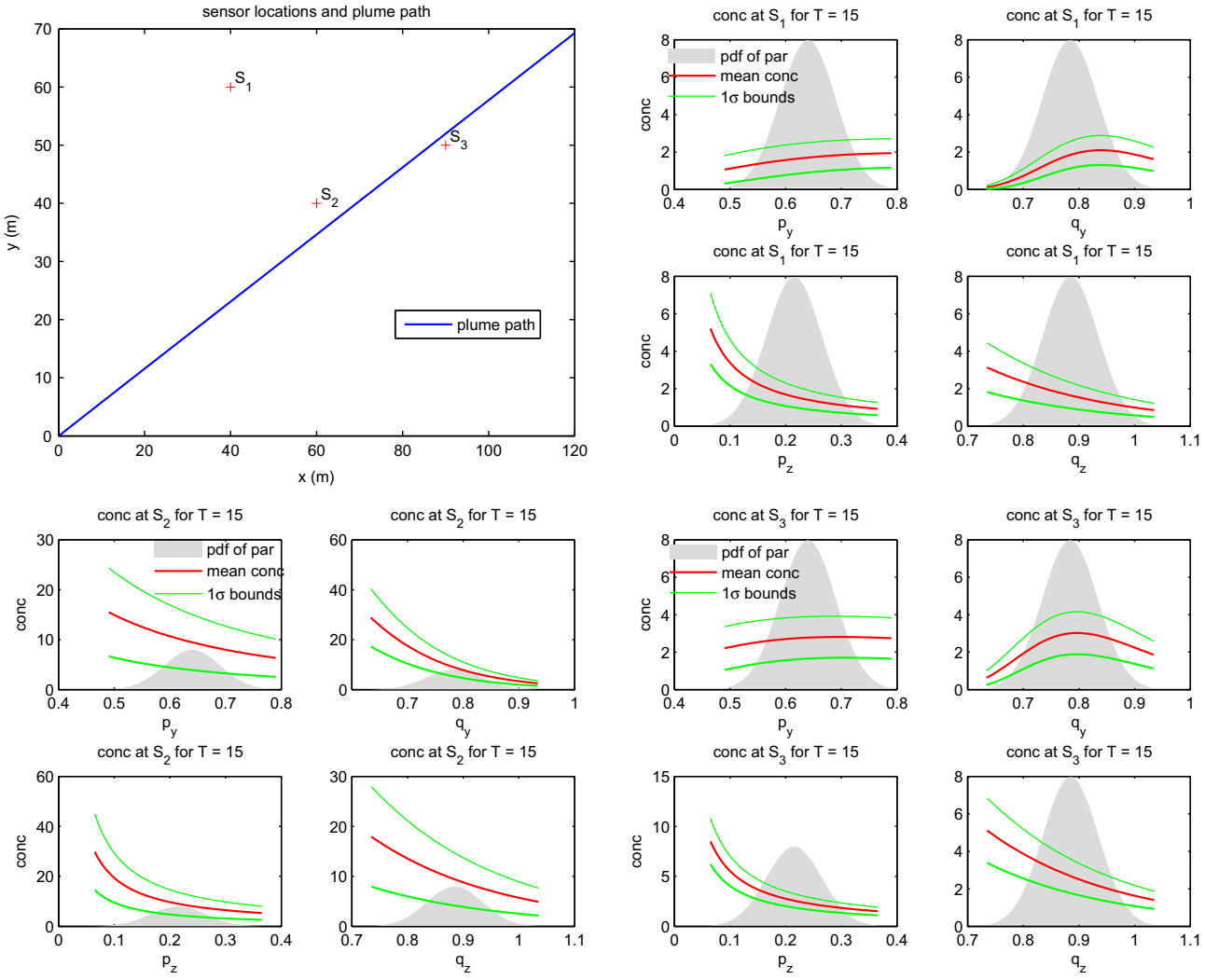

Fig. 5. Sensitivity of concentration w.r.t. normally distributed diffusion parameters.

approach is to approximate the stochastic system states in terms of a finite-dimensional series expansion in the infinite-dimensional stochastic space. The completeness of the space allows for the accurate representation of any random variable, with a given probability density function (*pdf*), by a suitable projection on the space spanned by a carefully selected basis. The basis can be chosen for a given *pdf*, to represent the random variable with the fewest number of terms. For example, the Hermite polynomial basis can be used to represent random variables with Gaussian distribution using only two terms. For dynamical systems described by parameterized models, the unknown coefficients are determined by minimizing an appropriate norm of the residual.

Let us consider a dynamical system of the form:

$$\mathrm{x}(k+1;\mathbf{p}) = \mathrm{f}(\mathrm{x}(k),\mathbf{u};\mathbf{p}) \tag{4}$$

where, $\mathrm{x}(k;\mathbf{p}) \in \mathbb{R}^n$ represents the stochastic system state vector at time step k, $\mathbf{u}$ represents the deterministic input and $\mathbf{p} \in \mathbb{R}^m$ represents the vector of uncertain system parameters, which is a function of a random vector ξ, with components ξ_j having a known *pdf* $g(\xi_\mathrm{j})$, with common support Ω. Now, each of the uncertain states and parameters can be expanded approximately by the finite-dimensional Wiener–Askey polynomial chaos (Xiu and Karniadakis, 2002) as:

$$x_\mathrm{i}(k,\mathbf{p}) = \sum_{r=0}^{P} x_{\mathrm{ir}}(k)\phi_\mathrm{r}(\xi) = \mathrm{x}_i^T(k)\Phi(\xi) \tag{5}$$

$$p_\mathrm{i}(k,\xi) = \sum_{r=0}^{P} p_{\mathrm{jr}}\phi_\mathrm{r}(\xi) = \mathbf{p}_j^T\Phi(\xi) \tag{6}$$

The total number of terms in the expansion is $P+1$ and is determined by the chosen highest order (l) of the polynomials $\{\varphi_\mathrm{r}\}$ and the dimension (m) of the vector of uncertain parameters p.

$$P+1 = \frac{(l+m)!}{l!m!} \tag{7}$$

3.1. Example

For a dynamical system with two independent uncertain parameters, each of which is a Gaussian random variable $\square(\mu_j, \sigma_j^2)$ for $j = 1, 2$, Hermite polynomials are chosen as the random orthogonal basis functions for expansion. Each of the uncertain parameters is expressed as a function of an independent Gaussian random variable $\xi_j \in \square(0,1)$. The orthogonal polynomials used in

Please cite this article in press as: Konda, U., et al., Uncertainty propagation in puff-based dispersion models using polynomial chaos, Environ. Model. Softw. (2010), doi:10.1016/j.envsoft.2010.04.005

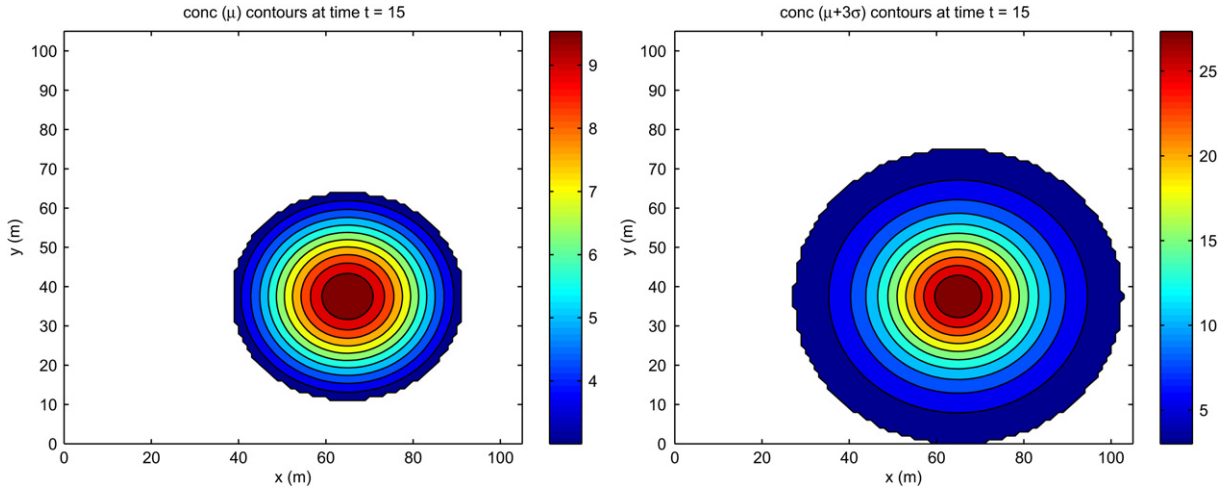

Fig. 6. Concentration ($C > 3$) field at $T = 15$.

the polynomial chaos expansion are constructed as the tensor products of 1-D Hermite polynomials in the $\xi 1$, $\xi 2$ space, the joint *pdf* of the random variables being given by:

$$P + 1 = \frac{(l+m)!}{l!m!} \tag{8}$$

The resulting orthogonal polynomials up to order l are given by:

$$\phi(\xi_1, \xi_2) = \phi_i(\xi_1)\phi_j(\xi_2),$$
$$\forall i = 0, 1, \ldots, l, \quad j = 0, 1, \ldots, l, \quad \text{where } i + j \leq l.$$

The Hermite polynomials up to, say, order $l = 2$ can be written as:

$$\begin{aligned}
\phi_0(\xi_1, \xi_2) &= 1 \\
\phi_1(\xi_1, \xi_2) &= \xi_1 \\
\phi_2(\xi_1, \xi_2) &= \xi_2 \\
\phi_3(\xi_1, \xi_2) &= \xi_1^2 - 1 \\
\phi_4(\xi_1, \xi_2) &= \xi_1\xi_2 \\
\phi_5(\xi_1, \xi_2) &= \xi_2^2 - 1
\end{aligned}$$

where each ξ_i is $N(0,1)$. Note that there are six terms in the expansion as given by Eq. (7). The system states can be written as:

$$x_i(t; \xi_1, \xi_2) = \sum_{r=0}^{5} x_{ir}(t)\phi_r(\xi_1, \xi_2), \text{for } i = 1, \ldots, n \tag{9}$$

The two uncertain parameters can be expanded as:

$$p_j(\xi_1, \xi_2) = \mu_j + \sigma_j\xi_j, \text{ for } j = 1, 2 \tag{10}$$

Note that the coefficients for the other terms are all zero.

3.2. Solution

Substitution of the approximate expressions for x and p in Eq. (5) and Eq. (6), in Eq. (4) leads to:

$$\begin{aligned}
&e_i(\xi) = \mathbf{x}_i^T(k+1)\Phi(\xi) - f_i(\mathrm{x}_1(k), \ldots, \mathrm{x}_n(k), \mathrm{u}, \mathrm{p}_1, \ldots, \mathrm{p}_m; \Phi(\xi)) \\
&\text{for } i = 1, \ldots, n
\end{aligned} \tag{11}$$

where, $e(\xi)$ represents the error due to the truncated polynomial chaos expansions of x and p. The $n(P + 1)$ time-varying unknown coefficients x_{ir} can be obtained using the Galerkin projection method. Projecting the error onto the space of basis functions $\{\varphi_r\}$ and minimizing it leads to $n(P + 1)$ deterministic ordinary difference equations:

$$\begin{aligned}
&\langle e_i(\xi), \phi_r(\xi)\rangle = 0 \\
&\text{for } \quad i = 1, \ldots, n \text{ and } r = 0, \ldots, P
\end{aligned} \tag{12}$$

where $\langle u(\xi), v(\xi)\rangle = \int u(\xi)v(\xi)g(\xi)d\xi$ represents the inner product induced by *pdf* $g(\xi)$.[Ω] For linear and polynomial functions, these integrals can be easily evaluated analytically (Ghanem and Spanos, 1991) to obtain the difference equations. For non-polynomial nonlinearities, these integrals represent a challenge. Numerical quadrature methods are used to evaluate the multi-dimensional integrals in the present work. For instance, Gauss–Hermite quadrature formulae may be used to evaluate the integrals for a Hermite polynomial basis. These quadrature methods fall under the broader

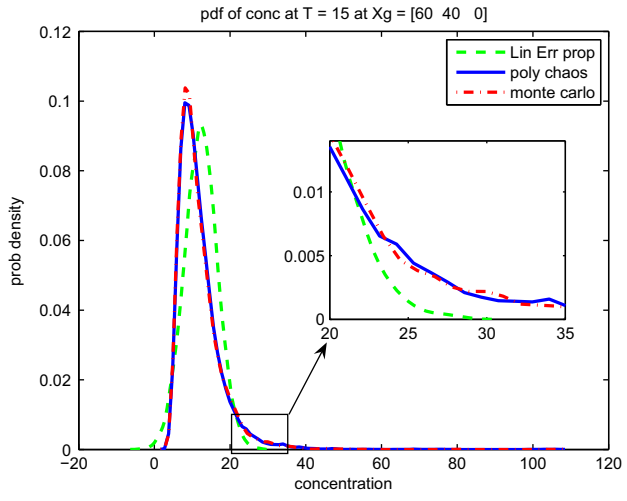

Fig. 7. *pdf* of concentration for normally distributed uncertainties.

Table 1
Uniform distribution bounds of diffusion parameters.

p_j	a_j	h
p_y	0.64	0.84
%	0.75	0.85
p_z	0.16	0.26
p_z	0.75	1

Please cite this article in press as: Konda, U., et al., Uncertainty propagation in puff-based dispersion models using polynomial chaos, Environ. Model. Softw. (2010), doi:10.1016/j.envsoft.2010.04.005

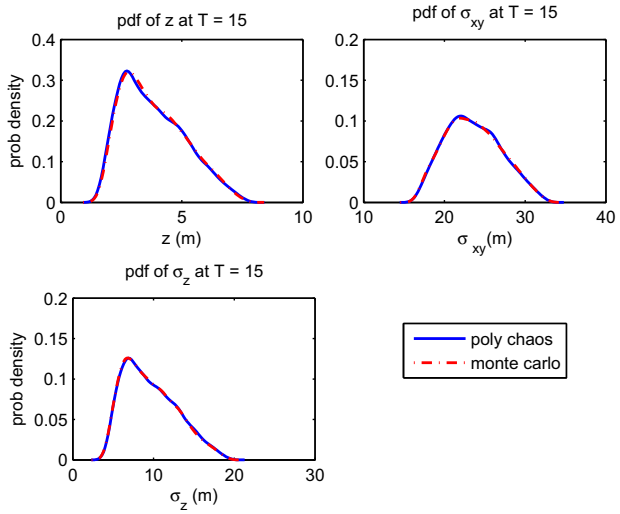

Fig. 8. *pdf* of uncertain states for uniformly distributed uncertainties.

sampling-based Non-Intrusive Spectral Projection (NISP) methods discussed in Reagan et al. (2003). The differential equations can then be solved to obtain the time-history of the time-varying coefficients x_{ir}. The solution of the stochastic system in Eq. (4) can thus be obtained in terms of polynomial functionals of random variables ξ_i:

$$x_i(k,\mathbf{p}) = \sum_{r=0}^{P} x_{ir}(k)\phi_r(\boldsymbol{\xi}), i = 1,\ldots,n$$

This expression can be used to estimate the *pdf* of the solution by Monte Carlo sampling of the random variables. Further, the first coefficient $x_{i0}(k)$ represents the mean of the solution $x_i(k,\mathbf{p})$ when $\varphi_0(\xi) = 1$. The other coefficients similarly represent the combinations of various moments of the solution:

$$x_{ir}(k) = \frac{\langle x_i(k,\mathbf{p}),\phi_r(\xi)\rangle}{\langle \phi_r(\xi),\phi_r(\xi)\rangle} = \frac{\int_{\mathbb{R}^m} x_i(k,\xi),\phi_r(\xi)g(\xi)d\xi}{\int_{\mathbb{R}^m} \phi_r^2(\xi)g(\xi)d\xi} \quad (13)$$

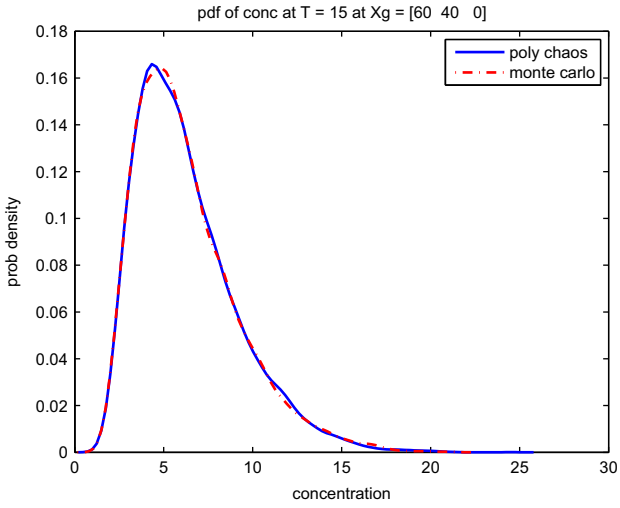

Fig. 9. *pdf* of concentration for uniformly distributed uncertainties.

The mean of the solution $x_i(k,\xi)$ can be easily calculated using the equation

$$\mathbf{E}[x_i(k,\mathbf{p}(\xi))] = \mu = \int_{\Omega} x_i(k,\mathbf{p}(\xi))g(\xi)d\xi \quad (14)$$

and the higher central moments by the equation:

$$\mathbf{E}\left[(x_i(k,\mathbf{p}(\xi)) - \mu)^n\right] = \int_{\Omega} (x_i(k,\mathbf{p}(\xi))^n)g(\xi)d\xi \quad (15)$$

4. Results and discussion

In the present work, the effects of uncertainties in diffusion parameters p_y,q_y,p_z and q_z and in initial location $[x_0,y_0]$ of the source on the solution of the dispersion model are studied in a simulated CBR dispersion scenario. The simulation experiments are performed for a plume evolution whose target species activity for each puff is 5×10^5. The units of activity can be chosen according to the species under study. Note that the units of concentration (as well as concentration error) are then *ActivityUnits*/m^3 in the following. The results are shown for two scenarios:

- Single puff release with parametric uncertainty, no initial location uncertainty and a fixed wind field at all locations
- Multiple puff release with parametric and initial location uncertainties, and wind varying with location

These scenarios and parameters for the simulations are next described.

4.1. Single puff release

The release occurs at the origin. The wind direction is 240° (measured clockwise from North) and blows horizontally across the domain at 5 m/s. The evolution of the 5 states of the puff is shown in Fig. 1, for the following diffusion parameters to determine the growth of a puff:

$$\begin{aligned} p_y &= 0.640, \quad q_y = 0.784 \\ p_z &= 0.215, \quad q_z = 0.885 \end{aligned} \quad (16)$$

The evolution of the surface concentration (concentration at [x, y, 0]) due to the release is shown in Fig. 2, where the concentration surface and contour plots are shown for two time instants $t = 10$ and $t = 20$.

The effects of parametric uncertainty are discussed for the cases of normal and uniform distribution of the four diffusion parameters p_y, q_y, p_z and q_z. Since these parameters do not effect the evolution of X_k and Y_k, they are deterministic.

4.1.1. Normal distribution

The diffusion parameters are assumed to be normally distributed around the values chosen in Eq. (16), with a standard deviation of 0.05. The three uncertain puff states are expanded, as described in Eq. (9), in terms of Hermite polynomial functionals of $\xi \in \mathbb{R}^4$, each ξ_m being a random variable with distribution $N(0,1)$. The series expansion is done up to order l, chosen appropriately. The diffusion parameters are similarly expanded, as described in Eq. (10). These polynomial chaos expansions are substituted in Eq. (2) and Eq. (3). Using Galerkin approximation as in Eq. (11), a set of deterministic difference equations are obtained which can be solved to obtain the solution of the stochastic system.

The resulting *pdf*s of the states are plotted for each of the uncertain states in Fig. 3, with the probability density along the

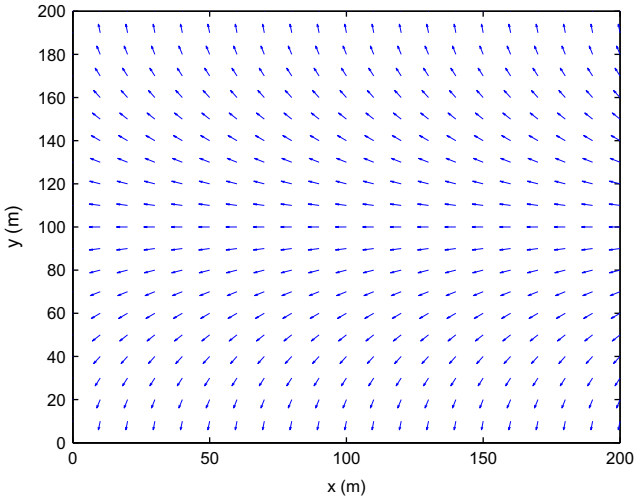

Fig. 10. Wind field across the domain.

vertical axis. These are compared with the *pdf*s obtained by the Monte Carlo solution, which involves solving the stochastic system many times, each time with a sample of the diffusion parameters drawn from their uncertainty distributions. 10 000 sample draws are chosen in the current example. The polynomial chaos approach involves fewer computations than the standard Monte Carlo approach while it can be seen that the approach captures the distribution of all the states as well as the Monte Carlo approach.

The *pdf* of each uncertain state is plotted using the MATLAB® function *ksdensity* which computes the probability density estimate using a normal kernel smoothing method. The function takes the Monte Carlo realizations of the uncertain state as the input to obtain the density estimate.

The concentration can be obtained by substituting the polynomial chaos solution in Eq. (1). In Fig. 4, the error in polynomial chaos solution is shown, at the grid location [20,10,0] for time $T = 15$. The absolute error in mean and variance respectively, is plotted by comparing with the solution obtained by solving the system for 50 000 Monte Carlo runs. The error is plotted for the polynomial chaos series expansion up to order 4, and for the 10 000 run Monte Carlo solution. It can be seen that the error decreases with increase in the order for the polynomial chaos solution. In all our examples, the polynomial chaos solution is for order 4, and the Monte Carlo solution is for 10 000 runs.

The polynomial chaos solution gives the joint effect of all the uncertain parameters on the concentration. The effect of a single parameter, ξ_j on the solution $y(\xi)$ can be captured using the moment equations:

$$\mu^j = \int_{\Omega} y(\xi) g(\xi_1, \ldots, \xi_{j-1}, \xi_{j+1}, \ldots, \xi_m) d\xi \tag{17}$$

μ^j being the mean, and the higher central moments μ_k^j:

$$\mu_k^j = \int_{\Omega} \left(y(\xi) - \mu^j\right)^k g(\xi_1, .., \xi_{j-1}, \xi_{j+1}, .., \xi_m) d\xi \tag{18}$$

The variation of the concentration with each of the uncertain diffusion parameters is shown in Fig. 5, for three different grid locations S_1, S_2 and S_3 at time $T = 15$. The three locations are chosen such that S_2 is near the puff center at that time, S_1 is away from the puff center on a line orthogonal to the plume path and S_3 away from the puff center but, along the plume path. The effect of each of the 4 uncertain diffusion parameters p_y,q_y,p_z, q_z is shown for each of the 3 locations, by plotting the mean and one standard deviation (1σ) bounds of the concentration values. The *pdf* of each of the parameters is also shown in the background. It can be seen from the plots that the mean concentration is higher for all the 3 grid locations, for smaller values of the diffusion parameters p_z and q_z, which correspond to diffusion in the z-direction. However, the concentration variation with p_y and q_y depend on the grid locations. For locations S_1 and S_3 away from the puff center, smaller values of diffusion in the xy-direction means the puff has not diffused to those locations at that time instant. Therefore, higher values of the diffusion parameters mean an expanded puff causing an increase in the

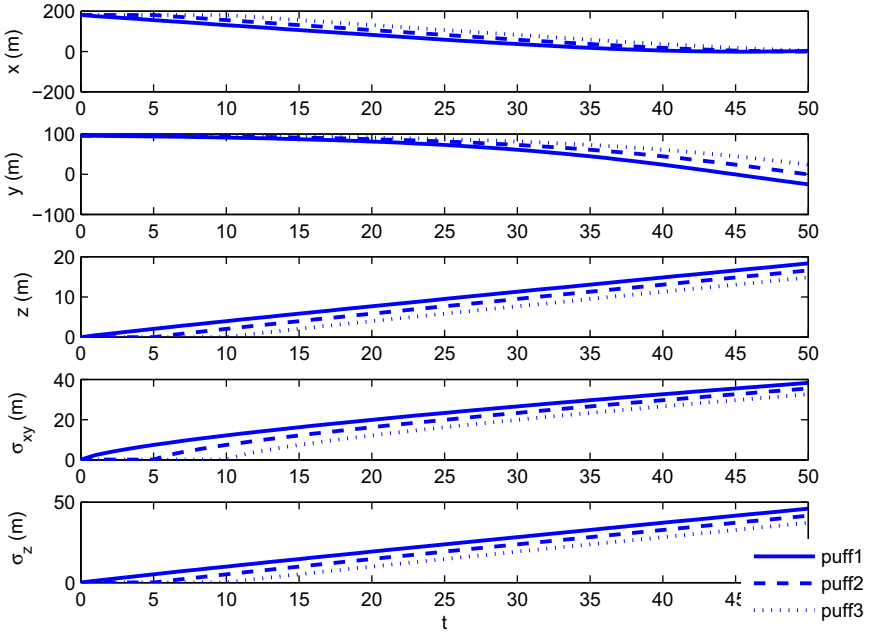

Fig. 11. Evolution of puff states.

Please cite this article in press as: Konda, U., et al., Uncertainty propagation in puff-based dispersion models using polynomial chaos, Environ. Model. Softw. (2010), doi:10.1016/j.envsoft.2010.04.005

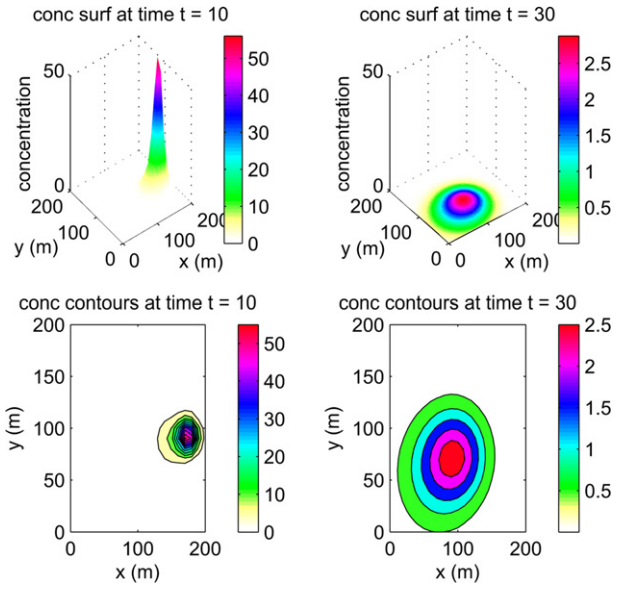

Fig. 12. Evolution of concentration.

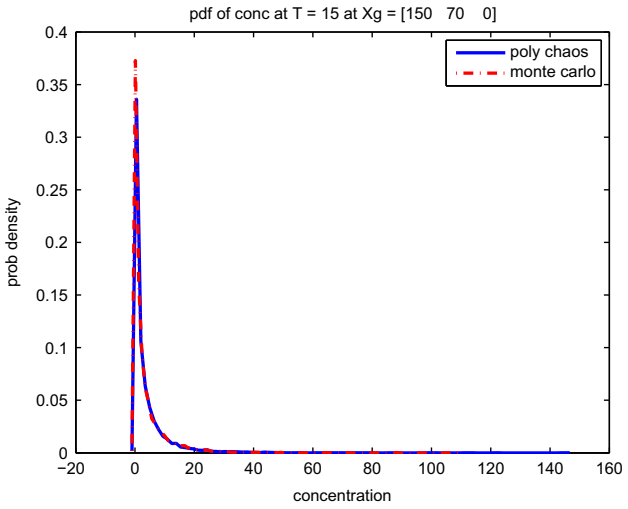

Fig. 14. *pdf* of concentration for normally distributed uncertainties.

mean concentration. A further increase in diffusion leads to dissipation and reduction in the concentration values. For location S_2, which is near the puff center, smaller diffusion parameters lead to higher concentrations as expected. The 1σ bounds are larger for larger mean concentration values in all scenarios.

In Fig. 6, the concentration contours at time $T = 15$ are plotted across the domain, for concentration values greater than a given threshold, which is chosen as 3 in this example. The first plot shows the mean (μ) concentration contours whereas the second plot shows the contours of concentration mean plus three standard deviations taking the uncertainty into account. The second plot gives a more realistic estimate of the hazard map to the decision-maker, compared to the one generated using just the expected concentration. Tracking the higher moments in addition to the mean is very important in such scenarios.

The *pdf* of the concentration at time $T = 15$ for grid location [60,40,0], is compared with that obtained from Monte Carlo solutions of the system in Fig. 7. It can be seen from the figure that the result is consistent with the Monte Carlo solution. In the same Fig. 7, the *pdf* of the concentration, obtained using the mean and variance

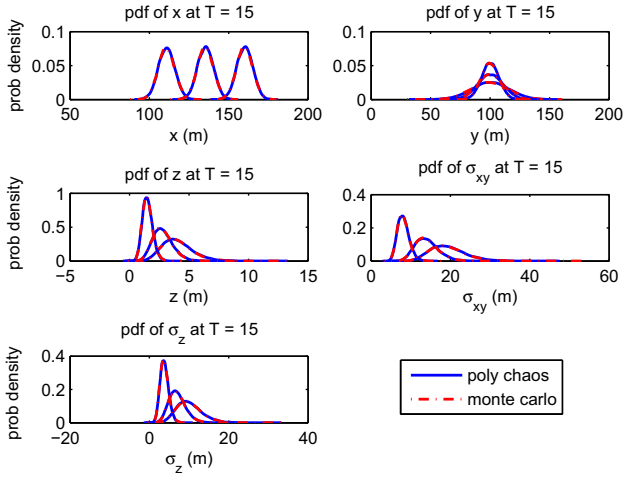

Fig. 13. *pdf* of uncertain states for normally distributed uncertainties.

information propagated using a linearized error model of the system, is also plotted (see the green dashed line). Since this method propagates only the mean and covariance, the true distribution is approximated with a Gaussian. It can be seen that the nonlinearities in the model and concentration equation cause the true *pdf* to be very different from this result. For instance, while the estimated mean concentration values are 9.51 for the true Monte Carlo solution and 9.6 for the polynomial chaos solution, the same for the solution obtained using linearized error propagation model is 12.25. Further, it can be seen from the magnified section of Fig. 7, that this approximation gives a negligible probability for concentrations above 25, while the *pdf* obtained from Monte Carlo/polynomial chaos approach gives a significant probability to influence the risk assessment of a decision-maker. In a CBR scenario, a decision-maker might order an evacuation based on the more accurate risk assessment or take other protective measures such as requiring first responders to wear protective gear, while not doing so using a less accurate method propagating only low order moments. This illustrates the limitations of the linearization approach, and propagating only the mean and covariance of the distribution.

4.1.2. Uniform distribution

The diffusion parameters are assumed to be uniformly distributed in this case. The bounds $[a_j, b_j]$ of the distribution of each of the parameters are as shown in Table 1.

The three uncertain puff states are expanded, in terms of Legendre polynomial functionals of $\xi \in \mathbb{R}^4$, each ξ_m being a random variable with distribution $U(-1,1)$. The series expansion is done up to order 4. The diffusion parameters are similarly expanded as follows:

$$p_j(\xi) = \frac{b_j - a_j}{2} + \frac{b_j - a_j}{2}\xi_j, \quad \text{for} \quad j = 1,\ldots,4$$
$$\text{where}, \quad p_j \in \square(a_j, b_j)$$

These polynomial chaos expansions are substituted in Eq. (2) and Eq. (3). Using Galerkin projection as in Eq. (11), a set of deterministic difference equations are obtained which can be solved to obtain the solution of the stochastic system. The resulting *pdf*s of the states are plotted for each of the uncertain states in Fig. 8, and compared with the *pdf* of the Monte Carlo solutions. It can be seen that the polynomial chaos approach captures the distribution of all states as well as the Monte Carlo approach. The highly skewed

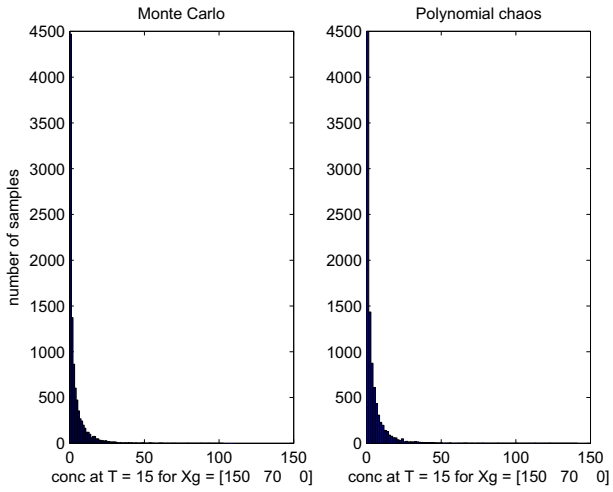

Fig. 15. Histograms of concentration for normally distributed uncertainties.

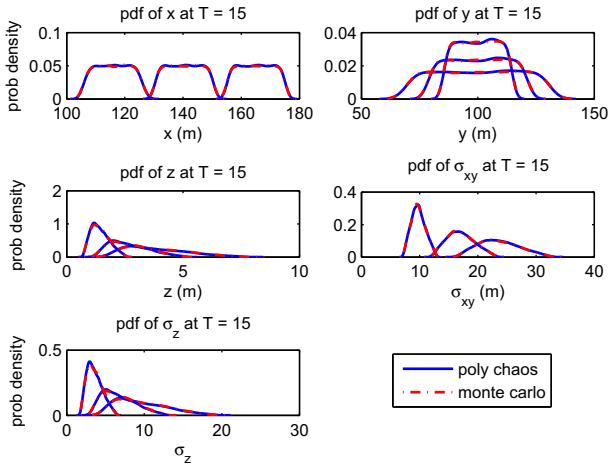

Fig. 16. *pdf* of uncertain states for uniformly distributed uncertainties.

non-Gaussian nature of the *pdf*s is well captured. This confirms that in addition to the mean and variance, the higher moments are also well captured by the PC expansion.

The uncertain concentration at a grid point at various time instants can then be obtained, as mentioned earlier, by substituting the polynomial chaos solution in Eq. (1). The resulting *pdf* of the concentration is compared with that obtained from Monte Carlo solutions of the system in Fig. 9.

The results show the ability of the method to accurately propagate the *pdf* of the uncertain states through nonlinear dynamics, for a wide variety of uncertainty distributions in the model parameters. The same approach is similarly valid for the propagation of initial condition uncertainties in the states, as illustrated in the following.

4.2. Multiple puff release

In this case, there are three puff releases from the source, one each at 0 s, 5 s and 10 s. The location of the source is uncertain and is around [200,100]. The wind speed across the domain is 5 *m*/*s* with varying direction dependent on the location as shown in Fig. 10. The evolution of the five states of each of the three puffs is shown in Fig. 11, for the diffusion parameters in Eq. (16).

The evolution of the surface concentration (concentration at [x, y, 0]) due to the release is shown in Fig. 12, where the concentration surface and contour plots are shown for two time instants $t = 10$ and $t = 30$. It is to be noted that the figure shows one particular realization of possible puff paths. Depending on the initial location of the sources, the puff paths could be north-ward or south-ward because of the varying wind direction with location.

The effects of parametric and initial condition uncertainties are discussed for the cases of normal and uniform distribution of the four diffusion parameters p_y,q_y,p_z and q_z and initial location [x_0,y_0].

4.2.1. Normal distribution

The diffusion parameters are assumed to be normally distributed around the values chosen in Eq. (16), with a standard deviation of 0.05. The initial location is assumed to be normally distributed with mean [185,100,0] and standard deviation [5,5,0]. In this case, the locations of each of the puffs in the evolution of the plume are also uncertain. The polynomial chaos expansions are done in terms of Hermite functionals, as described in the earlier section and a set of deterministic difference equations are obtained which can be solved to obtain the solution of the stochastic system. The initial condition uncertainties in the source location translate into the corresponding initial conditions of the deterministic set of equations.

Table 2
Uniform distribution bounds of source location.

x	a_j	b_j
x_0	180	200
y_0	90	110
z_0	0	0

The resulting *pdf*s of the states are plotted for each of the uncertain states in Fig. 13. These are compared with the *pdf*s obtained by the Monte Carlo solution, which involves solving the stochastic system several times, each time with a sample of the diffusion parameters and initial location drawn from their uncertainty distributions. The polynomial chaos approach performs well in capturing the propagated distribution.

The *pdf* (obtained using the MATLAB *ksdensity* function) of the uncertain concentration at a particular grid point (in this case [150,70,0]) is compared with that obtained from Monte Carlo solutions of the system in Fig. 14. The histograms of the same are shown in Fig. 15. It can be seen from the figures that the result agrees with the Monte Carlo solution.

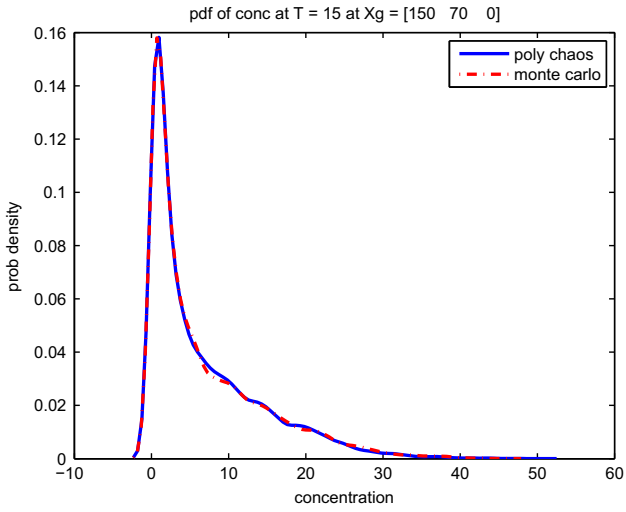

Fig. 17. *pdf* of concentration for uniformly distributed uncertainties.

Please cite this article in press as: Konda, U., et al., Uncertainty propagation in puff-based dispersion models using polynomial chaos, Environ. Model. Softw. (2010), doi:10.1016/j.envsoft.2010.04.005

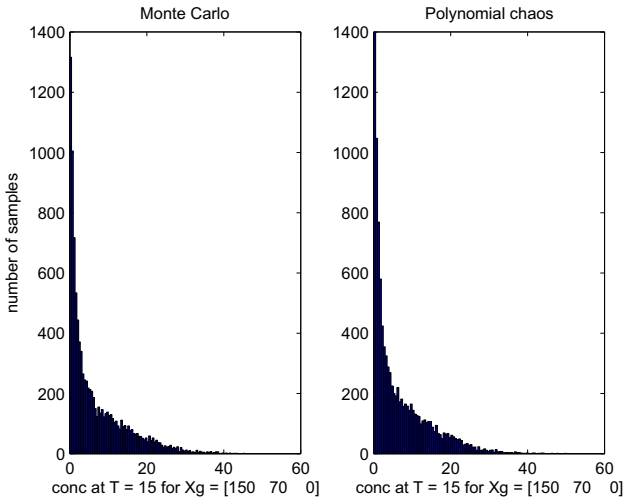

Fig. 18. Histograms of concentration for uniformly distributed uncertainties.

4.2.2. Uniform distribution

The diffusion parameters and the uncertain source location are assumed to be uniformly distributed in this case. The distribution of diffusion parameters is same as earlier, as shown in Table 1. The bounds $[a_j, b_j]$ of the distribution of each of the source location parameters are as shown in Table 2.

All the five puff states for each puff are expanded, in terms of Legendre polynomial functionals as described earlier, and a set of deterministic difference equations are obtained which can be solved to obtain the solution of the stochastic system. The initial condition uncertainties in the source location translate into the corresponding initial conditions of the deterministic set of equations.

The resulting *pdf*s of the states are plotted for each of the uncertain states in Fig. 16, and compared with the *pdf*s of the Monte Carlo solutions. It can be seen that the polynomial chaos approach captures the non-Gaussian distribution of all states, closely following the Monte Carlo approach.

The *pdf* of the uncertain concentration at [150,70,0] is similarly compared with that obtained from Monte Carlo solutions of the system in Fig. 17. The histograms of the same is shown in Fig. 18. It can be seen from the figure that the result agrees with the Monte Carlo solution. Note that the *pdf* obtained using the MATLAB *ksdensity* function in Fig. 17 seems to have support for negative concentrations, only because of the approximation using normal kernels.

These results illustrate the ability of the generalized polynomial chaos method to accurately quantify the evolution of parametric and initial condition uncertainties.

5. Conclusion

A three-dimensional puff-based dispersion model has been tested for the purpose of accurately estimating the uncertainty distribution of the solution, caused by propagation of the uncertainty in the diffusion parameters and initial conditions of the model. The polynomial chaos approach is discussed in this context. An approximate solution to the stochastic system is obtained as a linear combination of the selected orthogonal basis functionals, whose coefficients are functions of time.

The polynomial chaos approach has been used to study the effect of each of the diffusion parameters on the output concentration at various spatial locations. Using this approach, the solution to the stochastic nonlinear dynamical system is obtained in terms of functionals of random variables, in terms of which the true distribution and moments of the solution can be approximated. The polynomial chaos solution is shown to compare well with the ground truth, determined by Monte Carlo simulation. The polynomial chaos approach involves fewer computations than the standard Monte Carlo solution approach which requires solving the dynamical model many times for many realizations of the uncertain parameters. Improved estimates of the higher order moments of the output concentration distribution give a more realistic estimate of the hazard maps to the decision-maker, in case of harmful releases into the atmosphere. When measurements are available, this information about the distribution of the propagated solution can be used to make predictions with improved accuracy using data assimilation. This suggests an extension of this approach to filtering problems with dynamical models having known parametric uncertainty distributions, a task currently under investigation.

Acknowledgment

This work is supported under contract no. HM1582-08-1-0012 from ONR.

References

ASG-TRC, 2003. The CALPUFF modeling system. http://www.src.com/calpuff/calpuff1.htm.

Cameron, R.H., Martin, W.T., 1947. The orthogonal development of non-linear functionals in series of Fourier–Hermite functionals. The Annals of Mathematics 48 (2), 385–392.

Cheng, H., Sandu, A., 2009. Uncertainty quantification and apportionment in air quality models using the polynomial chaos method. Environmental Modelling & Software 24 (8), 917–925.

EPA, 2005. Dispersion modeling. http://www.epa.gov/scram001/dispersionindex.htm.

Errico, R.M., 1997. What is an Adjoint model? Bulletin of the American Meteorological Society 78, 2577–2591.

EUJRC, 2004. Features of dispersion models. http://rem.jrc.ec.europa.eu/etex/37.htm.

Ghanem, R., Red-Horse, J., 1999. Propagation of probabilistic uncertainty in complex physical systems using a stochastic finite element approach. Physica D: Nonlinear Phenomena 133 (1–4), 137–144.

Ghanem, R.G., Spanos, P.D., 1991. Stochastic Finite Elements: A Spectral Approach. Springer-Verlag, New York, NY.

Helton, J., Johnson, J., Sallaberry, C., Storlie, C., 2006. Survey of sampling-based methods for uncertainty and sensitivity analysis. Reliability Engineering & System Safety 91 (10–11), 1175–1209.

Holmes, N., Morawska, L., 2006. A review of dispersion modelling and its application to the dispersion of particles: an overview of different dispersion models available. Atmospheric Environment 40, 5902–5928.

IAEA, 1989. Evaluating the reliability of predictions made using environmental transfer models. http://www-pub.iaea.org/mtcd/publications/PubDetails.asp?pubId=3703.

Isukapalli S.S., 1999. Uncertainty Analysis of Transport-Transformation Models. Ph. D. thesis. Rutgers, The State University of New Jersey.

Isukapalli, S., Roy, A., Georgopoulos, P., 1998. Stochastic response surface methods (SRSMs) for uncertainty propagation: application to environmental and biological systems. Risk Analysis 18 (3), 351–363.

Knio, O.M., Le Maître, O.P., 2006. Uncertainty propagation in CFD using polynomial chaos decomposition. Fluid Dynamics Research 38, 616–640.

Najm H.N. Uncertainty quantification and polynomial chaos techniques in computational fluid dynamics. Annual Review of Fluid Mechanics 41(1).

National Research Council (U.S.), 2003. Committee on the Atmospheric Dispersion of Hazardous Material Releases, Tracking and Predicting the Atmospheric Dispersion of Hazardous Material Releases: Implications for Homeland Security. National Academies Press.

Rao, K.S., 2005. Uncertainty analysis in atmospheric dispersion modeling. Pure and Applied Geophysics 162, 1893–1917.

Reagan, M.T., Najm, H.N., Ghanem, R.G., Knio, O.M., 2003. Uncertainty quantification in reacting-flow simulations through non-intrusive spectral projection. Combustion and Flame 132 (3), 545–555.

Rood, A.S., McGavran, P.D., Aanenson, J.W., Till, J.E., 2001. Stochastic estimates of exposure and cancer risk from carbon tetrachloride released to the air from the rocky flats plant. Risk Analysis 21, 675–696 (22).

Sandu, A., Sandu, C., Ahmadian, M., 2006. Modeling multibody dynamic systems with uncertainties. Part I: Theoretical and computational aspects. Multibody System Dynamics 15 (4), 369–391.

Sykes, R., Parker, S., Henn, D., Cerasoli, C., Santos, L., 1998. PC-SCIPUFF Version 1.2PD Technical Documentation. Tech. Rep. ARAP Report No. 718. Titan Research and Technology Division, Princeton, NJ.

Terejanu, G., Singla, P., Singh, T., Scott, P.D., 2008. Uncertainty propagation for nonlinear dynamic systems using Gaussian mixture models. Journal of Guidance, Control and Dynamics 31 (6), 1623–1633.

Thykier-Nielsen, S., Deme, S., Mikkelsen, T., 1999. Description of the Atmospheric Dispersion Module RIMPUFF. Tech. Rep. RODOS(WG2)-TN(98)-02. Riso National Laboratory, Roskilde, Denmark.

Whelpdale, D.M., 1991. Methods for assessing exposure of human and non-human biota. In: Geographically-Placed Atmospheric Models. John Wiley and Sons Ltd..

Wiener, N., 1938. The homogeneous chaos. American Journal of Mathematics 60 (4), 897–936.

Xiu, D., Karniadakis, G.E., 2002. The Wiener–Askey polynomial chaos for stochastic differential equations. SIAM Journal on Scientific Computing 24 (2), 619–644.

Zannetti, P., 1990. Air Pollution Modeling: Theories, Computational Methods and Available Software. Van Nostrand Reinhold, New York, NY, p. 167.

Please cite this article in press as: Konda, U., et al., Uncertainty propagation in puff-based dispersion models using polynomial chaos, Environ. Model. Softw. (2010), doi:10.1016/j.envsoft.2010.04.005